

PROBING THE EVOLUTION OF EARLY-TYPE CLUSTER GALAXIES THROUGH CHEMICAL ENRICHMENT

IGNACIO FERRERAS & JOSEPH SILK¹

Nuclear & Astrophysics Lab. 1 Keble Road, Oxford OX1 3RH, United Kingdom

To be published in The Astrophysical Journal.

ABSTRACT

A simple chemical enrichment model for cluster early-type galaxies is described in which the main mechanisms considered in the evolutionary model are infall of primordial gas, outflows and a possible variation in the star formation efficiency. We find that — within the framework of our models — only outflows can generate a suitable range of metallicities needed in order to explain the color-magnitude relation. The chemical enrichment tracks can be combined with the latest population synthesis models from Bruzual & Charlot (1999) to simulate clusters over a wide redshift range, for a set of toy models with different infall rates, star formation efficiencies and star formation scenarios. The color-magnitude relation of local clusters is used as a constraint, fixing the correlation between absolute luminosity and ejected fraction of gas from outflows. It is found that the correlations between color or mass-to-light ratios and absolute luminosity are degenerate with respect to most of the input parameters. However, a significant change between monolithic and hierarchical models is predicted for redshifts $z \gtrsim 1$. The most important observable that differentiates between these alternative formation scenarios is the population of blue early-type galaxies which fall conspicuously blueward of the red envelope. The comparison between predicted and observed mass-to-light ratios yield an approximate linear bias between total and stellar masses: $M_{\text{Tot}} \propto M_{\text{St}}^{1.15 \pm 0.08}$ in early-type galaxies. If we assume that outflows constitute the driving mechanism for the colors observed in cluster early type galaxies, the metallicity of the intracluster medium (ICM) can be linked to outflows: the color-magnitude constraint requires faint $M_V \sim -16$ galaxies to eject 85% of their gas, which means that most of the metals in the ICM may have originated in these dwarf galaxies. No significant evolution is predicted, in agreement with X-ray observations (Mushotzky & Loewenstein 1997). Other mechanisms contributing to the enrichment of the ICM such as ejected material from mergers that formed the largest ellipticals should be translated into a decrease of the intracluster metallicity at $z \gtrsim 1 - 1.5$. Forthcoming observations from *Chandra* and *XMM* will help elucidate this point.

Subject headings: galaxies: evolution — galaxies: formation — galaxies: elliptical — galaxies: clusters

1. INTRODUCTION

Almost eighty years after the famous Great Debate between Curtis and Shapley on the distance scale to spiral nebulae (Trimble 1995), many issues in extragalactic astronomy have been solved. However, one of the most basic properties, namely the star formation history in galaxies, is still a matter of controversy. We only have a qualitative description that separates early-type from late-type galaxies. The spectrophotometry-dynamics connection still waits to be established and the mechanism responsible for tight correlations found in early-type galaxies such as the Fundamental Plane, the Color-Magnitude relation (CM) or the Magnesium-central velocity dispersion correlation still remains a mystery. While galaxies in rich clusters only contribute around 5% to the total number in the Universe (Bahcall 1996), they live in a high density environment which provides a more advanced counterpart to field galaxy evolution (notwithstanding cluster specific issues such as interactions with the hot intracluster medium). All galaxies in a given cluster lie approximately at the same distance, which makes the distribution in apparent and absolute luminosities the same, allowing observations of a reasonably large and unbiased sample. Even though we cannot infer from actual data that all cluster galaxies are coeval (i.e. a monolithic formation scenario), their evolution can also be traced — on average —

by comparing clusters at different redshifts.

The study of the stellar populations in galaxies is complicated by the presence of degeneracies, the most extreme of which is that between age and metallicity (Worthey 1994). The effect of age or metallicity on many spectrophotometric observables is very similar: for instance, a set of colors or spectral indices can be associated either with an old population of stars with a low metal content or with a young population with higher metallicity. A recent analysis of a sample of clusters from Stanford, Eisenhardt & Dickinson (1998) with redshifts $0 < z < 1$ showed that the constraints from multi-band (optical and near-infrared) color-magnitude relations still allow a wide range of formation redshifts, as low as $z_F \sim 1$ for the faint end of the observed red envelope (Ferreras, Charlot & Silk 1999). More targeted spectral indices such as Balmer absorption or the study of the mass-to-light ratios show better age sensitivity, but the effect of metallicity combined with the large uncertainties usually found in actual observations thwarts any reliable estimation of the age distribution of the stellar populations. The age-metallicity degeneracy thereby allows the possibility of additional mechanisms in order to explain the tight scaling relations found in early-type galaxies other than a naive assumption of a highly synchronous process of monolithic collapse in which the age spread of the stellar populations is very small. A highly stable process in the evolution of ellipticals could result in a

¹Also at Department of Astronomy and Physics, University of California, Berkeley CA 94720

“conspiracy” that entangles age and metallicity in such a way that the stellar populations have a wide range of ages while keeping the correlations as tight as observed. Unfortunately, this very freedom complicates estimates of the star formation history in galaxies, especially early types, for which the major tracers of star formation are absent, leaving only the imprint of the slowly-evolving population of intermediate and low mass stars in their spectral energy distribution.

A model-dependent way of breaking the age-metallicity degeneracy involves a chemical enrichment prescription, which combines the simplified treatment of galaxy evolution by the use of a star formation rate and an adopted distribution of stellar masses as they are born (the initial mass function) along with our knowledge of stellar evolution and nucleosynthesis. The most severe uncertainties come from the yields, i.e. the mass fraction of stars transformed into metals for a given mass, caused by the difficulties in modelling such stellar evolution processes as stellar winds, mixing, the extremely high sensitivity of nuclear cross sections to the temperature, and the process of core collapse in high mass stars. This makes any attempt at tracing the abundances of single elements a qualitative rather than quantitative issue, and prompted our simplification of the model, tracing only the net metallicity of the galaxy, i.e. the fraction of elements other than hydrogen or helium. In §2 and 3 this model is described in detail as well as the simulation of the population of early-type galaxies in a cluster. In §4, 5 and 6 we explore the predicted color-magnitude, M/L vs mass relation and magnesium versus central velocity dispersion, respectively, for a set of enrichment toy models as well as for a few star formation scenarios. Section 7 is devoted to describing a possible estimator of cluster evolution through the population of blue early-type galaxies. Section 8 analyzes the enrichment of the intracluster medium from galaxy ejecta, fundamental to the model presented in this paper. Finally, Section 9 discusses the principal conclusions.

2. A RECIPE FOR CHEMICAL ENRICHMENT

In order to study the chemical enrichment of early-type galaxies in clusters we will follow the formalism of Tinsley (1980), reducing the model to a set of a few parameters that govern the evolution. A two-component system is considered, consisting of cold gas and stars. Only the net metallicity will be traced, i.e. all elements heavier than helium count in the same way. A more precise setup where the abundances of different elements are computed is beyond the scope of this project, which aims at finding the most basic mechanisms responsible for the observed range in metallicities that gives rise to the tight correlations obeyed by early-type galaxies, such as the color-magnitude relation. The mass in stars ($M_s(t)$) and in cold gas ($M_g(t)$) are normalized to the initial gas mass:

$$\mu_s(t) \equiv \frac{M_s(t)}{M_g(t=0)} \quad (1)$$

$$\mu_g(t) \equiv \frac{M_g(t)}{M_g(t=0)}. \quad (2)$$

We assume instantaneous mixing of the gas ejected by stars as well as instantaneous cooling of the hot gas component. The metallicity $Z(t)$ represents the average metal content of the different stellar populations comprising the galaxy. The final spectral energy distribution comprises the integration of stellar populations with different ages “modulated” by the star formation

rate, and with an average metallicity given by the chemical enrichment equations. Although recent observations of moderate redshift clusters hint at high formation redshifts $z_F \gtrsim 3$ (e.g. Ellis et al 1997; Stanford et al. 1998), the age-metallicity degeneracy is still capable of explaining the colors of the faintest $z \sim 0$ galaxies (below L_*) with a formation redshift as low as $z_F \sim 1$ (Ferreras et al. 1999). The basic physics related to chemical enrichment is reduced to a few mechanisms, namely:

- **Infall:** Accretion of gas from outside is needed in order to explain the G-dwarf problem (Van den Berg 1962; Schmidt 1963). Exponential infall at low metallicity is assumed: $f(t) = \Theta(t - \tau_{lag}) A_{inf} e^{-(t - \tau_{lag})/\tau_{inf}}$, where $\Theta(x)$ is the step function. The parameters ($A_{inf}, \tau_{inf}, \tau_{lag}$) regulate the infall rate, timescale and delay, respectively. These infall parameters are constrained by the metallicity distribution of old disk stars (e.g. Prantzos & Silk 1998).
- **Outflows:** Outflows triggered by supernovae explosions (SNe) constitute another important factor contributing to the final metallicity of the galaxy (Larson 1974, Arimoto & Yoshii 1987). Hence we define a parameter B_{out} which represents the fraction of gas that is ejected from the galaxy. Eventually this parameter should be a function of the mass of the galaxy, whose potential well determines whether the SNe winds are strong enough to escape the pull of gravity. The outflow fraction is constrained by the deuterium abundance as well as the metallicity distribution of old disk stars (Scully et al. 1997; Cassé et al. 1998).
- **Star Formation Efficiency:** A linear Schmidt law (Schmidt 1963) is assumed: $SFR(t) \equiv \psi(t) = C_{eff} M_g(t)$, where the parameter C_{eff} gives the star formation efficiency, which should depend — among other things — on the mass of the galaxy as well as on whether a bursting episode is taking place. We will not worry here about a steeper, non-linear Schmidt law that may be required to account for the observed deuterium abundances (Cassé et al. 1998), or for a possible enhancement of the star formation rate with metallicity (Talbot & Arnett 1975).

The aim of this chemical enrichment prescription is to break the degeneracy between age and metallicity — in a strongly model-dependent way — so that the large regions in (Age, Metallicity) space which are compatible with the CM relation observed in early-type cluster galaxies can be constrained (Ferreras et al. 1999). The input parameters are only five: ($A_{inf}, \tau_{inf}, \tau_{lag}, B_{out}, C_{eff}$), with some additional initial values which are: the initial metallicity and mass of stars and gas, the Initial Mass Function (IMF) slopes and cutoffs, as well as the metallicity of the infall gas. We will fix them hereafter to the following values:

- $\mu_s(t=0) = 0$
- $Z_g(t=0) = Z_f = 10^{-4}$
- Scalo IMF (Scalo 1986) with cutoffs at 0.1 and $100 M_\odot$.

The equations can be separated into one that follows the mass evolution and a second that traces chemical enrichment.

2.1. Mass Evolution

The evolution of the mass in gas and stars is given by:

$$\frac{d\mu_g}{dt} = (1 - B_{out})E(t) - C_{eff}\mu_g(t) + \Theta(t - \tau_{lag})A_{inf}e^{-(t - \tau_{lag})/\tau_{inf}} \quad (3)$$

$$\frac{d\mu_s}{dt} = C_{eff}\mu_g(t) - E(t) \quad (4)$$

$$E(t) = \int_{m_t}^{\infty} dm \phi(m)(m - w_m)C_{eff}\mu_g(t - \tau_m). \quad (5)$$

The integral $E(t)$ is the mass in gas ejected at time t from stars which have reached the end of their lifetimes. τ_m is the lifetime of a star with mass m . The Instantaneous Recycling Approximation (IRA) is a simple relation for the lifetimes of stars, frequently used in analytic calculations (e.g. Tinsley 1980), which reduce τ_m to either zero or infinity depending on the mass cut. This considerably simplifies the calculation without having a huge effect on the final metallicities, and is justified by the fact that massive stars ($M \gtrsim 10M_{\odot}$) provide most of the metals and have lifetimes roughly 1000 times shorter than stars with solar masses, whose chemical contribution is negligible in comparison. However, we will solve the equations numerically. Hence we will use actual lifetimes obtained from a broken power law fit to the data from Tinsley (1980) and Schaller et al (1992):

$$\left(\frac{\tau_m}{Gyr}\right) = \begin{cases} 9.694 \left(\frac{M}{M_{\odot}}\right)^{-2.762} & M < 10M_{\odot} \\ 0.095 \left(\frac{M}{M_{\odot}}\right)^{-0.764} & M > 10M_{\odot} \end{cases} \quad (6)$$

m_t is the turnoff mass, i.e. the mass of a main sequence star which reaches the end of its lifetime at a time t . Finally, w_m is the stellar remnant mass for a star with main sequence mass m :

$$\left(\frac{w_m}{M_{\odot}}\right) = \begin{cases} 0.1(m/M_{\odot}) + 0.45 & m/M_{\odot} < 10 \\ 1.5 & 10 < (m/M_{\odot}) \leq 25 \\ 0.61(m/M_{\odot}) - 13.75 & m/M_{\odot} > 25 \end{cases} \quad (7)$$

The mass for white dwarf remnants was taken from Iben & Tutukov (1984). The $1.5M_{\odot}$ remnant mass given for the intermediate range is the average mass of a neutron star (e.g. Shapiro & Teukolsky 1983), whereas supernovae from heavier stars might give birth to black holes, locking more mass into remnants (Woosley & Weaver 1995).

2.2. Chemical Enrichment

The equations for the evolution of the metallicity of the gas and the stars are:

$$\begin{aligned} d(Z_g\mu_g)/dt &= -C_{eff}Z_g(t)\mu_g(t) + \Theta(t - \tau_{lag})Z_f A_{inf}e^{-(t - \tau_{lag})/\tau_{inf}} + \\ &+ (1 - B_{out})E_Z(t) \end{aligned} \quad (8)$$

$$\begin{aligned} d(Z_s\mu_s)/dt &= C_{eff}Z_g(t)\mu_g(t) - \\ &- C_{eff} \int_{m_t}^{\infty} dm \phi(m)(m - w_m - mp_m)(Z_g\mu_g)(t - \tau_m) \end{aligned} \quad (9)$$

$$\begin{aligned} E_Z(t) &= \int_{m_t}^{\infty} dm \phi(m)C_{eff}[(m - w_m - mp_m)(Z_g\mu_g)(t - \tau_m) + \\ &+ mp_m\mu_g(t - \tau_m)], \end{aligned} \quad (10)$$

where $\phi(m)$ is the initial mass function (IMF). The fraction of a star of mass m transformed into metals is given by p_m , and is simplified by a triple power law (with cuts at 0.7 and $1.0M_{\odot}$) using the yields from Renzini & Voli (1981) and Marigo, Bressan & Chiosi (1996) for Intermediate Mass Stars (IMS) (i.e. $M \lesssim 10M_{\odot}$). More massive stars undergo supernova explosions which generate a large amount of metals. The yields in this mass range are taken from Woosley & Weaver (1995) and Thielemann, Nomoto & Hashimoto (1996). Rather important uncertainties arise because of the complicated shock wave that is generated during core collapse. Usually a cutoff mass is assumed so that all matter above it is ejected into the interstellar medium. The differences in the yields between these two groups are due to the different physical inputs assumed, mainly the criterion for convection, the nuclear reaction rates, and the determination of the mass cut

Type Ia supernovae should also be considered as they contribute a large fraction of iron. These SNe are assumed to originate in a binary system in which at least one of the stars is a white dwarf. The infall of gas from the companion pushes the mass above the Chandrasekhar limit, triggering a deflagration with the subsequent disruption of the star. The thermonuclear burning during this process generates roughly $0.7M_{\odot}$ of iron for a $1M_{\odot}$ $C + O$ white dwarf (W7 model of Thielemann, Nomoto & Yokoi 1986). We use the ratio of Type Ia to Type II (i.e. core collapse) supernovae rates $N(Ia)/N(II) = 0.12$ from Nomoto, Iwamoto & Kishimoto (1997), in order to quantify the number of Type Ia's that explode at a given time. This estimation is based on a best fit to known solar abundances, and so the ratio might be different for early-type galaxies. However, this approximation is valid in the regime where early types have a high star formation rate, i.e. during the first few million years when the rate of type II supernovae is significant. In the worst case, this approximation will translate into a systematic underestimate of the iron yield whose effect will be diminished by the imposed color-magnitude constraint. The equations are integrated using a fifth-order Runge-Kutta method with adaptive stepsize control given by the Cash-Karp prescription (Press et al. 1992). The integration does not find any special numerical hurdle as all functions entering the differential equations are smooth power laws. Only some rescaling was necessary, changing the step scale from linear to logarithmic when computing the mass integrals in order to achieve convergence with a small number of steps.

The evolution of the metallicity for a range in all five parameters ($A_{inf}, \tau_{inf}, \tau_{lag}, B_{out}, C_{eff}$) is shown in figure 1, where the (Age, Metallicity) regions for the brightest ($2L_*$) and faintest ($L_*/4$) bins of the early-type cluster population of a cluster at $z \sim 0.5$ are overlaid (Ferreras et al. 1999). The main conclusion that can be drawn from the chemical enrichment tracks is that galaxy outflows (B_{out}) constitute the principal driving mechanism for generating a suitable range of metallicities that can explain the tight correlations in early-type galaxies such as the Color-Magnitude relation. With respect to infall of gas: neither the rate (A_{inf}), timescale (τ_{inf}) nor delay (τ_{lag}) can change the metallicities significantly unless pre-enrichment of the infall gas ($Z_f >> 10^{-4}$) or a time dependence $Z_f(t)$ for its metal content are assumed. Needless to say, the final mass in stars and gas can be greatly changed by infall, but the metallicity is roughly the same. A range of star formation efficiencies (C_{eff}) will only change the timescale to reach some asymptotic final metallicity which is the same regardless of the value of C_{eff} .

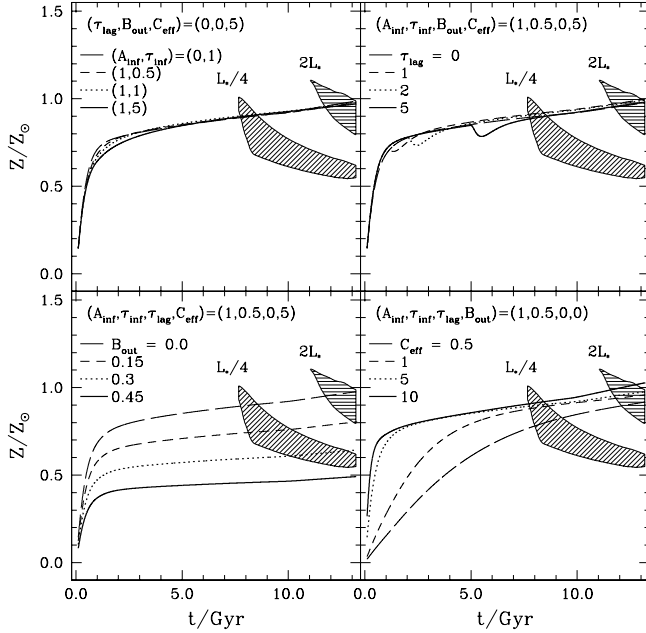


FIG. 1.— Chemical enrichment tracks overlaid on the age and metallicity regions for two luminosity bins — corresponding to $2L_*$ and $L_*/4$ — for cluster Cl0016+16 ($z = 0.545$) using Color-Magnitude constraints (Ferreras et al. 1999). Different ranges of infall are shown in the upper panels: Infall rate and timescale (A_{inf} and τ_{inf} , respectively, left), and Infall delay (τ_{lag} in Gyr, right). The bottom right panel shows the chemical enrichment tracks for a range of star formation efficiencies (C_{eff}), whereas the bottom left panel plots the evolution of metallicity for a few ejected fractions (B_{out}). Only this one is capable of generating a suitable range of metallicities that yields the color range of the red envelope.

This final metallicity depends on more basic factors such as the shape of the IMF or the yields from massive stars. Hence, if we want to avoid any unphysical fine tuning in the galaxy formation process in order to explain the CM relation, we conclude that outflows from SNe-triggered winds are the main cause of the observed range of metallicities in early-type cluster galaxies. Since the ejected fraction parameter B_{out} is mainly related to the mass of the galaxy, we could even extend this statement to field early-type galaxies.

Figure 2 shows a mapping of the enrichment tracks shown in figure 1 into a color-age diagram, where restframe $U-V$ color is plotted versus formation redshift (bottom panels). Throughout this paper, the translation between ages and redshifts is done using an open cosmology with $\Omega_0 = 0.3$ and $H_0 = 60 \text{ km s}^{-1} \text{ Mpc}^{-1}$. The shaded area encompasses the range of $U-V$ colors observed in the Coma cluster (Bower, Lucey & Ellis 1992, BLE92). Even though figure 2 shows that a range in infall parameters or star formation efficiency could explain the observed color range, one should take into account the star formation rate: the top panels trace the star formation rate through the equivalent width of $\text{H}\alpha$ using the standard prescription (e.g. Kennicutt 1998). The choices of parameters that yield the bluest colors of observed early-type cluster galaxies ($U-V \sim 1.2$) imply a non-negligible $\text{H}\alpha$ emission line for a wide range of formation redshifts and thus must be ruled out. The dotted horizontal line sets an observational upper limit $\text{EW}(\text{H}\alpha) < 0.5 \text{ \AA}$ below which all realistic models should lie. Hence, models with large amounts of infall, long infall delays or low star formation efficiencies are not considered.

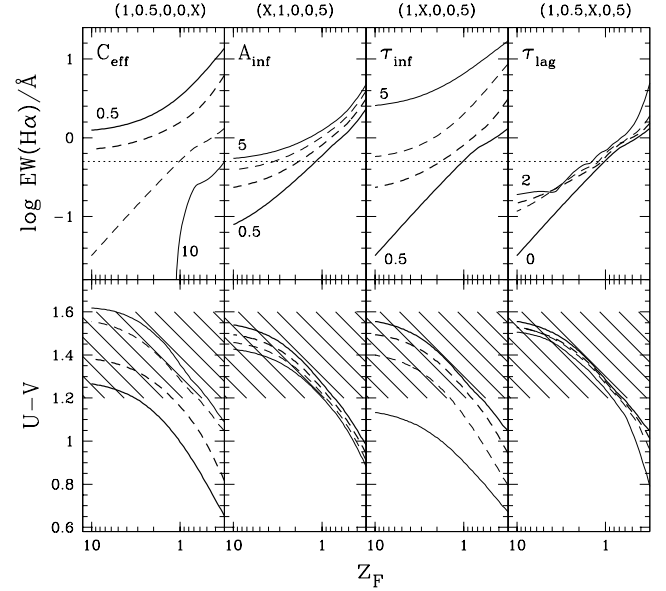


FIG. 2.— Bottom Panels: Projection of chemical enrichment tracks on rest frame $U-V$ color vs. formation redshift. An open cosmology with $\Omega_0 = 0.3$ and $H_0 = 60 \text{ km s}^{-1} \text{ Mpc}^{-1}$ is used to translate between ages and redshifts. The shaded region encompasses the color range found in local clusters such as Coma or Virgo. Top Panels: Equivalent widths of $\text{H}\alpha$ from the computed star formation rate (SFR) (see text for details). Some of the models can be ruled out as they would predict detectable emission lines in nearby early-type cluster galaxies. The leftmost panel shows the star formation efficiency (C_{eff}) must be high to avoid this. The numbers on top label the parameters used for each trajectory as $(A_{\text{inf}}, \tau_{\text{inf}}, \tau_{\text{lag}}, B_{\text{out}}, C_{\text{eff}})$ with X meaning several values for that parameter are considered.

Models that satisfy this constraint must have a high star formation efficiency which implies a strong and short-lived burst of star formation, in agreement with the standard scenario.

2.3. Analytic Approximation

An analytic solution to a simplified version of the chemical enrichment equations can illustrate the importance of outflows in the final metallicities. Let us assume the Instantaneous Recycling Approximation with stellar lifetimes 0 and ∞ separated at some mass cutoff M_0 . Let us also consider no infall. In this case, the integration of the gas mass equations (3) and (5) is an exponential decay:

$$\mu_g(t) = e^{-t/T_g}, \quad (11)$$

where $T_g^{-1} = C_{\text{eff}}[1 - R(1 - B_{\text{out}})]$, and R is the returned fraction of gas, i.e. $R = \int_{M_0}^{\infty} dm \phi(m)(m - w_m)$, dependent on the IMF. The metallicity of the gas can be readily solved from (8) and (10) giving:

$$Z_g(t) = 1 - e^{-\gamma t} \sim \gamma t, \quad (12)$$

where $\gamma = C_{\text{eff}}(1 - B_{\text{out}})(1 - R)y$, and $(1 - R)y = \int_{M_0}^{\infty} dm \phi(m)mp_m$, i.e. dependent both on the IMF and the stellar yields. The asymptotic behavior ($Z_g(t) \rightarrow 1$) is formally correct but physically meaningless, as the real equations should take into account the change of the yields with metallicity. We have assumed $Z_g(t) \ll 1$ for the approximation. Equations (11) and

(12) show that the final metallicities are of order:

$$\gamma T_g = \frac{(1-B_{out})(1-R)y}{1-(1-B_{out})R}, \quad (13)$$

and are independent of the star formation efficiency. This gives some sort of “effective yield” to which the metallicity will tend at late times, which depends on the IMF (through R , and y), the stellar yields (y) and the ejected fraction (B_{out}). These gas metallicities can be computed for a Salpeter and a Scalo IMF with a cutoff at $M_0 = 10M_\odot$, giving $2.4Z_\odot$ and $0.7Z_\odot$, respectively. A Salpeter IMF is flatter at the high mass end, which explains the higher metallicity. Hence, a change in the slope of the IMF can also reproduce the same metallicity range found for a range of outflows.

2.4. Caveats

Before venturing on the predictions generated by this simple chemical enrichment model, it is worth mentioning the most important uncertainties and simplifications which might contribute to changing the output. First and foremost, the large uncertainties in modelling stellar evolution result in large error bars in the yields (p_m) which will render any estimation of chemical evolution only believable on a qualitative basis regardless of the fine-tuning of the chemical enrichment prescriptions that are considered. This is what motivates a simple recipe that takes into account the most basic mechanisms driving chemical enrichment in galaxies, as well as tracing only the net metal content rather than following the abundance of single elements. The connection between ejected fractions and absolute luminosities should not be taken at face value but, rather, as a rough estimate. There are quite a few factors affecting the asymptotic metallicities (as seen in the previous section), such as changes in the IMF slope, the dependence of the stellar yields on metallicity (e.g. Portinari, Chiosi & Bressan 1998) or the metallic composition of the ejected winds if mixing is not perfect.

Finally, any non-primordial infall will add a degeneracy between infall parameters and ejected fractions: the infall of gas with a significant metal abundance will mimic the same enrichment tracks for primordial infall in galaxies with lower ejected fractions. However, if an anti-correlation between absolute luminosity and outflows is considered, then we could argue that such a mechanism will make some of the fainter galaxies as red as the brightest ones, thereby increasing the scatter about the color-magnitude relation.

Therefore, we emphasize that this model should be considered as a “back-of-the-envelope” numerical simulation, exploring an important region of the enormous volume of parameter space in the process of galaxy formation and evolution. In principle, the most fundamental processes are the ones considered in this paper, namely the role of outflows, infall of gas or a significant variation in the efficiency forming stars. The role of other mechanisms mentioned above and elsewhere (e.g. pre-enrichment, top-heavy IMFs or variable stellar yields) will be left for later study.

3. SIMULATING A CLUSTER

Once the chemical enrichment tracks have been computed for a single galaxy, the process can be extended to simulate the population of early-type galaxies in a cluster. A suitable connection between the ejected fraction (parameter B_{out}) and the

absolute luminosity is obtained by using the CM relation of a local cluster as a constraint. Hence, for a given value of the ejected fraction, the chemical enrichment model is used to infer a metallicity for a given age. Figure 3 shows the relation between luminosity, stellar mass and color vs. the ejected fraction as constrained by the color-magnitude relation of local clusters. The range of galaxies observed in the Coma cluster by Bower, Lucey & Ellis (1992), which corresponds to absolute luminosities $-23.5 < M_V < -19.5$ maps into a range of ejected fractions: $0 < B_{out} < 0.5$. The dependence of $U-V$ and $V-K$ colors with B_{out} is also plotted for a set of five toy models described in table 1. The fiducial model (A1) assumes no infall and a star formation efficiency of $C_{eff} = 10$. The other models include infall of gas. Model C has a reduced star formation efficiency and model D delays the infall 1 Gyr after the galaxy starts forming stars ($\tau_{lag} = 1$ Gyr). All these models are degenerate with respect to color, which can be explained with the enrichment tracks shown in figure 1: only parameter B_{out} yields a significant range of metallicities. So, these different models will just slightly “modulate” the enrichment tracks of the bottom left panel of figure 1.

As long as high enough formation redshifts are considered ($z_F \gtrsim 3$), we can assume a pure metallicity sequence for the local cluster that is used as a constraint. This approximation is very robust since more realistic non-pure metallicity sequences will still give the same metallicity range: figure 1 shows that after a few billion years the metallicity stays roughly constant: once the most massive stars ($M \gtrsim 10M_\odot$) have reached the end of their lives, chemical enrichment is controlled by the population of intermediate mass stars which have long lifetimes as well as low metal yields. For a given ejected fraction, we can read off the age and metallicity and — using the latest popu-

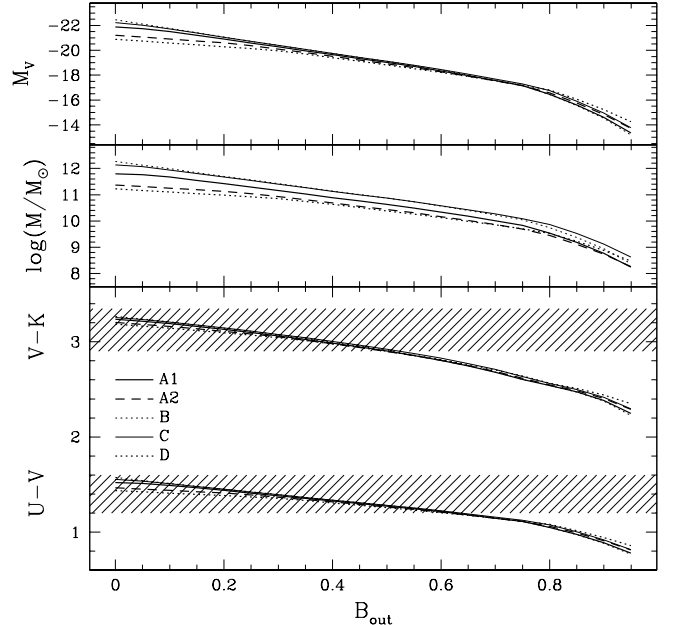


FIG. 3.— Evolution of V -band absolute luminosity, stellar mass, $U-V$ and $V-K$ color (both computed in the rest frame), with respect to the ejected fraction parameter — B_{out} — for a set of enrichment toy models (see table 1). The M_V evolution is just a mapping of the $U-V$ color curves, since the Color-Magnitude relation of the Coma cluster from Bower, Lucey & Ellis (1992) is used as constraint. The curves for all five toy models are degenerate, so that only parameter B_{out} is useful in order to identify the early-type galaxies along the red envelope sequence.

TABLE 1

Chemical Enrichment Toy Models

Model	A_{inf}	τ_{inf}	τ_{tag}	B_{out}	C_{eff}	Comments
<i>A1</i>	1	0.5	0	0–0.95	10	Default
<i>A2</i>	1	1	0	0–0.95	10	Extended Infall
<i>B</i>	0	—	—	0–0.95	10	No Infall
<i>C</i>	1	1	0	0–0.95	5	Low SF Efficiency
<i>D</i>	1	0.5	1	0–0.95	10	Delayed Infall

lation synthesis models from Bruzual & Charlot (1999) (hereafter BC99) — the rest frame $U-V$ color. Finally, the CM relation from BLE92 is considered in order to infer an absolute luminosity. The sample of galaxies is chosen to fit the the luminosity function of early-type (normal plus dwarf) galaxies in the Virgo cluster measured by Sandage, Binggeli & Tammann (1985), using a Schechter function with parameters $\alpha = -1.40$ and $M_V = -23.0$ (a translation from B to V band was performed assuming a color $B-V \sim 1.0$ for an early-type galaxy).

4. COLOR-MAGNITUDE RELATION

One of the most useful estimators of evolution in cluster early-type galaxies is the color-magnitude relation. The study of rest frame $U-V$ color versus absolute luminosity traces the change in the age and metallicity of the stellar populations. The small scatter found in clusters at low and moderate redshifts is an indicative sign of either a highly synchronous formation process or a very stable region in color-magnitude space.

Figure 4 shows the prediction of the CM relation at four different redshifts for the three star formation scenarios described in table 2: The M-model is a monolithic collapse process (e.g. Larson & Tinsley 1974), where the formation redshift of all early-type galaxies follows a Gaussian distribution with mean $z_F = 5$ and standard deviation $\sigma(z_F) = 1$, thus written as $M(5,1)$. The H-model represents a cluster in which most of the star formation in the brightest galaxies occur at late times compared to the faintest ones. This model cannot be directly related to a specific hierarchical clustering scenario (e.g. Kauffmann, White & Guiderdoni 1993), although it resembles a scenario where strong mergers take place in the brightest galaxies at late times, with a large fraction of stars being formed at lower redshifts, assumed to be $z_F \gtrsim 2$, whereas the faintest galaxies have formation redshifts $z_F \sim 10$. The correlation between luminosity and formation redshift is assumed to be linear and with a gaussian spread of $\sigma = 1$. The notation for this model is $H(2,10,1)$. We do not assume a major stage of star formation later than $z_F \sim 2$ as current observations of early-type cluster galaxies in a wide redshift range ($0 < z < 1$) seem to discard that possibility (e.g. Stanford et al. 1998).

Finally, the IH-model is an inverted hierarchical clustering process which corresponds to $H(10,2,1)$, i.e. the brightest galaxies are the first ones to form at $z_F \sim 10$. This type of evolution will occur if the first objects to form were to reheat the intergalactic medium, raising the Jeans mass so that the more massive galaxies form first (Blanchard, Valls-Gabaud & Mamon 1992). Table 2 also lists the time lapse over which star formation takes place in the cluster. A monolithic collapse model condenses this stage into 0.6 Gyr, whereas the H and IH models

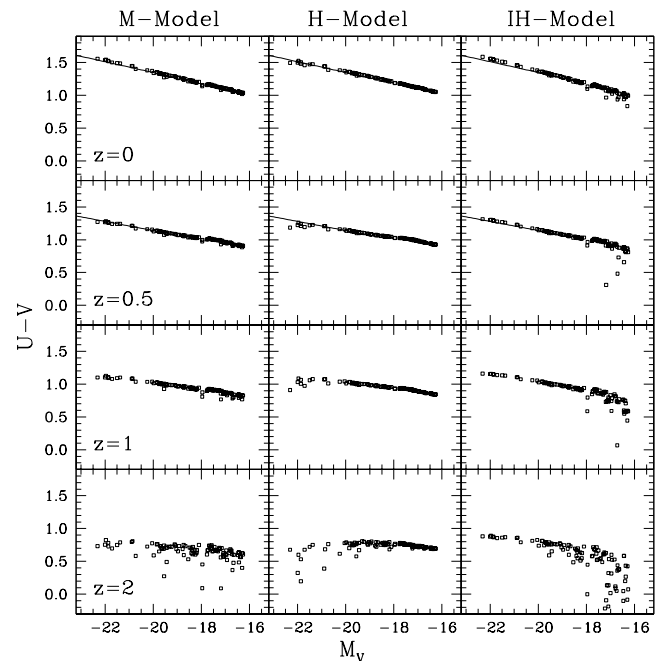


FIG. 4.— Simulation of the rest frame $U-V$ vs M_V color-magnitude relation of a cluster at different redshifts for three star formation models: Monolithic (M), Hierarchical (H) and Inverted Hierarchy (IH) (see table 2). The solid lines are linear fits to observed CM relations at $z \sim 0$ (Coma, Bower, Lucey & Ellis 1992) and $z \sim 0.5$ (Cl0016+16, Ellis et al. 1997). Notice the presence of blue outliers with respect to absolute luminosity at high redshift depends on the formation scenario: A “bottom-up” hierarchy could thus be tested by the observation of the bright end of the color magnitude relation in high redshift clusters.

extend the interval to 5 Gyr. Taking into account the luminosity function, the inverted hierarchy model implies a rather strong rate of star formation at low redshift. The difference between these three star formation scenarios can be seen in the CM predictions at four redshifts in figure 4. The solid lines are the linear fits to observed CM relations at $z \sim 0$ (Coma, BLE92), and at $z \sim 0.5$ (Cl0016+16, Ellis et al. 1997). One can see that these models are degenerate in clusters at low to moderate redshifts ($0 < z < 1$), taking into account observational uncertainties. However, both hierarchical scenarios will yield a significant population of blue outlier galaxies at redshifts $z > 1$. The monolithic model produces a “luminosity-blind” scatter that increases at high redshift blueward of the red envelope all along the luminosity sequence, whereas the H and IH models preferentially display outliers at the bright and faint ends, respectively of the “main sequence” red envelope. Thus, observations

Star Formation Scenarios

TABLE 2

Label	Model	$\Delta t_{SF}/\text{Gyr}$ ($\Omega_0 = 0.3; h_0 = 0.6$)	Comments
<i>M</i>	M(5,1)	0.60	Monolithic
<i>H</i>	H(2,10,1)	5.01	Hierarchical
<i>IH</i>	H(10,2,1)	5.01	Inverted Hierarchy

of high redshift clusters should easily confirm or rule out an ordered hierarchy — as opposed to a monolithic collapse — in the formation of the stellar populations with respect to the total luminosity of the galaxy. Notwithstanding possible dynamical processes that might have triggered the observed recent star formation, we can identify these blue galaxies as young spheroids with a significant population of A-type stars (there should be no massive OB stars as long as we assume a negligible star formation rate at $z < 2$), so that they will plausibly display the spectral feature of a post-starburst galaxy (also referred to as E+A or k+a) (Dressler & Gunn 1983), i.e. a spectrum of an old population of stars (E or k) with an added population of young stars (A) which will be characterized by strong Balmer absorption lines. This issue will be treated in more detail in §7 as this population can represent an important tracer of cluster evolution.

The main parameters of the CM relation (slope, zero point measured at the brightest cluster galaxy and the rms residuals about the linear fit) can be used to constrain the epoch of star formation in galaxies as well as the basic factors contributing to their evolution. Figures 5a and 5b show the evolution of the main CM parameters as a function of redshift both for several enrichment toy models (fig 5a) and for three star formation models (fig 5b). Figure 5a shows that a wide range of infall rates, timescales or infall delays as well as a stronger star formation efficiency result in no major change from the default model: an extension of the result shown for the evolution of rest frame $U - V$ color for a single galaxy with different chemical enrichment processes (fig 2). Only a large difference in ages will yield different slopes, zero points or residuals. However, the need for strong initial star formation rates imply a negligible difference between models unless redshifts very close to z_F are considered. Only an IH model yields significantly different residuals about the CM relation as well as a steeper slope at high redshift.

Also shown in these two figures are the observations of 17 clusters in the range $0.3 < z < 0.9$ from the sample of Stanford et al. (1998), corrected to rest frame “ $U - V$ ” versus absolute luminosity in the V -band. The translation was done by assuming passive evolution and a formation redshift $z_F = 5$ for all of the galaxies in each cluster. Notice the large scatter and error bars which render the estimation of star formation histories a rather qualitative quest until a large enough sample of cluster observations become available. The rms residuals from the observed sample can only yield weak limits on the intrinsic residuals from age and metallicity differences between galaxies. Photometric uncertainties overwhelm the intrinsic scatter unless high redshift clusters with a significant population of young galaxies are observed. Furthermore, the sample of

galaxies has only been culled with regard to morphology by using high resolution *HST/WFPC2* images, but no spectroscopic confirmation of cluster membership has been done for all the galaxies. Hence, a significant contamination from line-of-sight early-type galaxies can be expected. We should emphasize that the model residuals computed are a poor estimator of a hierarchical clustering process. In this scenario, the young outlier galaxies are the few brightest ones, which do not count as much towards the final residuals as the more numerous older and fainter population. Hence, luminosity-weighted residuals would be more useful for this purpose.

5. MASS-TO-LIGHT RATIOS

The stellar mass-to-light ratios can also be computed using the population synthesis models from BC99. The ratio of mass to luminosity is a very age-sensitive quantity, thereby making it one of the most useful observables for breaking the age and metallicity degeneracy. Unfortunately, observed M/L ratios have large uncertainties so that a large sample in a wide range of redshifts is necessary in order to discriminate between formation scenarios. Figures 6a and 6b show the predictions from our chemical enrichment model for the main parameters of the correlation between $\log M/L_V$ and $\log M$. A non-zero slope yields the tilt of the fundamental plane relative to the expectation using the virial theorem. A range of chemical enrichment toy models results in a degeneracy for the slope, zero point and residuals of this correlation. In analogy with the CM relation, these parameters are most sensitive to age differences as shown in figure 6b for three star formation scenarios. The middle panels show there is good agreement in the zero points with M/L observations measured for five clusters: Coma ($z = 0.02$), Cl1358+62 ($z = 0.33$), Cl0024+16 ($z = 0.39$), MS2053+03 ($z = 0.58$) and MS1054-03 ($z = 0.83$), obtained from the compilation of Van Dokkum et al. (1998). The trend with redshift gives a linear fit $\Delta \log M/L_V = -0.34z$ for the range $0 < z < 1$, in agreement with Van Dokkum et al. (1998), who find $\Delta \log M/L_B = -0.4z$. However, we can see in the figures that this evolution is not linear, and so a fit using a wider range of redshifts $0 < z < 2$ gives a flatter slope $\Delta \log M/L_V = -0.28z$. The residuals could represent a way of discerning the formation history, but given realistic values for the error bars, we doubt that cluster observations, at least in the redshift range $0 < z < 1$ could be used for this purpose.

A comparison of the slopes obtained with purely stellar masses — around $M/L_V \propto M^{0.075-0.085}$ for a monolithic model — with actual observations: $M/L \propto M^{0.15-0.25}$ (e.g. Mobasher et al. 1999) shows that stellar masses alone cannot account for this, and dark matter (DM) should therefore be included. The slope mismatch is caused by a correlation between stellar mass

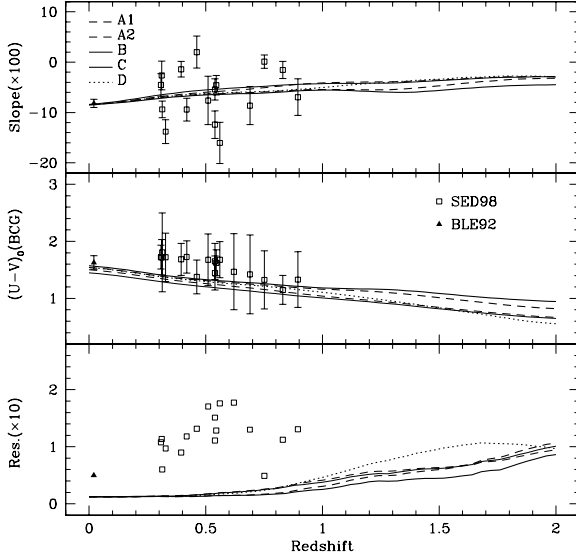
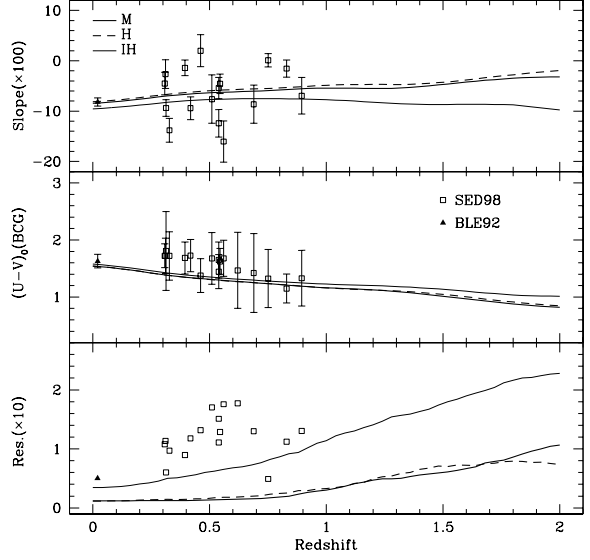


FIG. 5.— *a*) Evolution of the main parameters in the Color-Magnitude relation (slope, zero point evaluated at the brightest cluster galaxy and rms residuals) for a set of enrichment toy models. The points are cluster observations from Bower, Lucey & Ellis (1992) (triangle), and Stanford, Eisenhardt & Dickinson (1998) (squares). For SED98 we translated their colors (which used different filters depending on the cluster redshift to trace the 4000A break) to actual rest frame $U - V$, using passive evolution with a formation redshift $z_F = 5$ along with the models from Bruzual & Charlot (In preparation). The rms residuals from the observations should be taken with caution since cluster membership is not confirmed for all early-type galaxies observed in SED98. *b*) Same as figure 5a with respect to three different star formation scenarios: Monolithic (M), Hierarchical Clustering (H) and an Inverted Hierarchy (IH) (see table 2).

and dark matter, so that there is more invisible mass in galaxies with more mass in stars. Given that the model presented in this paper only gives the average, qualitative trend of different observables, we should only take these slopes as indicative. However, if we speculate that the actual mismatch between mass in stars and DM is similar to the one obtained here (i.e. between a slope of $\sim 0.15 - 0.25$ for DM and $\sim 0.075 - 0.085$ for stars), then the trend should be $M_{\text{DM}} \propto M_{\text{St}}^{\alpha}$, with $\alpha = 1.15 \pm 0.08$, i.e. the scaling between dark matter and luminous matter is roughly linear, which implies a mass-independent bias for ellipticals. This renders the studies of (stellar) M/L ratios using population synthesis models applicable to dynamical masses as well, with the proviso that an offset should be added when dealing with the total mass.

6. THE EVOLUTION OF THE MAGNESIUM ABUNDANCE

The abundance of magnesium traces the star formation history of the population of massive stars in the galaxy. It is strongly correlated with the central velocity dispersion (σ) which implies an enhanced star formation rate in more massive ellipticals. This correlation might possibly depend on the environment as found by Guzmán et al. (1992) and Jørgensen, Franx & Kjægaard (1996). Furthermore, there is an overabundance of magnesium in the cores of the brightest ellipticals which may imply an enhanced massive star formation rate in these regions. A solution to this overabundance would require an *ad hoc* correction factor as a function of absolute luminosity. In order not to introduce further uncertainties, we will simply show the predictions without any correction. Figure 7 shows the evolution with redshift of the Lick/IDS index Mg_2 (Worthey 1994) versus the logarithm of the central velocity dispersion ($\log \sigma$) for all three star formation scenarios considered in this



paper. The data points come from observations of local clusters by Guzmán et al. (1992, G92); Jørgensen et al. (1996, J96); Pahre, Djorgovski & de Carvalho (1998, P98); and Colless et al. (1999, EFAR), as well as from a few elliptical galaxies in clusters at $z \sim 0.37$ observed by Ziegler & Bender (1997, Z97). In this case, a slope cannot be obtained because of the small observational sample. Thus, the error bars instead give the range of observed magnesium abundances. The overabundance problem is readily seen in the zero point estimated at the brightest cluster galaxy, as well as in the predicted flatter slopes. A different age spread in the stellar populations among galaxies — expected for H and IH models at high redshift ($z \gtrsim 1$) — will translate into a large scatter, explained by the fact that Mg_2 is a strongly metallicity-dependent observable. Hence, at late times (when the metallicity is roughly constant with age) the magnesium abundance will be controlled by fixed parameters such as the stellar yields or the slope and cutoff of the upper mass segment of the IMF. Only the fraction of outflows will contribute to explain a range of abundances as a function of absolute luminosity (or velocity dispersion, via the Faber-Jackson relation). It is only at early stages — when the metallicity changes significantly with age — that we expect to find a noticeable difference among star formation scenarios.

7. BLUE OUTLIERS AS TRACERS OF CLUSTER EVOLUTION

Figure 4 shows that the presence of galaxies falling conspicuously blueward of the “main sequence” red envelope represents an important estimator for evolution in early-type cluster galaxies. This blueness is caused by the presence of young A-type stars associated with a recent star formation process. The main sequence lifetime of these stars translates into a time lapse of 1 to 4 Gyr after which the last important star formation

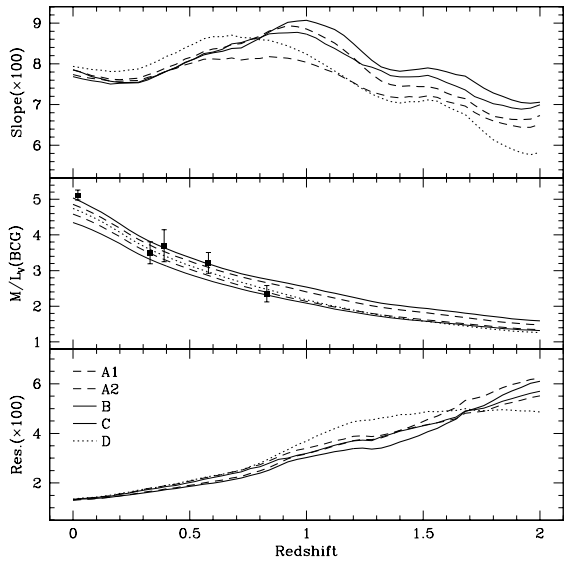
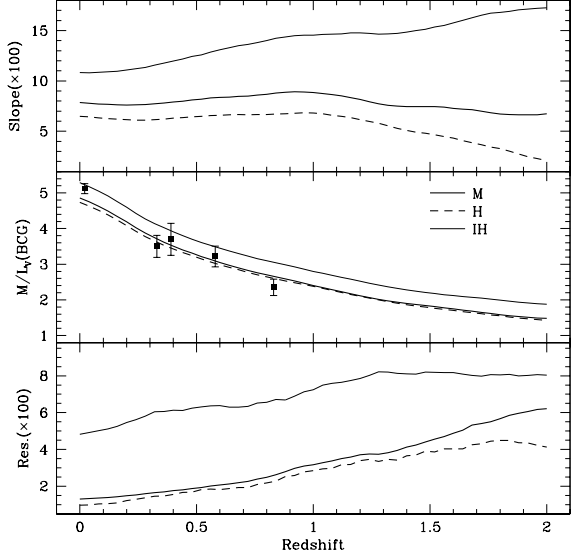


FIG. 6.— *a*) Evolution of the slope, zero point at the brightest cluster galaxy and residuals of the $\log(M/L_V)$ vs $\log M$ relation for a set of enrichment toy models. The points are values for several clusters: Coma ($z = 0.02$); Cl 1358+62 ($z = 0.33$); Cl 0024+16 ($z = 0.39$); MS 2053+03 ($z = 0.58$) and MS 1054-03 ($z = 0.83$) from the compilation of figure 3 from Van Dokkum et al. (1998). The slope — around 0.075 – 0.085 — for stellar mass-to-light ratios disagrees with actual observations of the TOTAL mass-to-light ratio (0.15 – 0.25 , e.g. Mobasher et al. 1999) which implies a correlation between total and stellar mass of order: $M_{\text{TOT}} \propto M_{\text{Stellar}}^{1.15 \pm 0.08}$ *b*) Same as figure 6a with respect to three different star formation scenarios (see table 2).

process ceased. This interval is correlated with the equivalent width of Balmer absorption lines. The lack of star formation is confirmed by the absence of emission lines from hot OB stars. Hence, the spectrum of these blue outlier galaxies would thus be classified as “E+A” (Dressler & Gunn 1983). Some of the brightest blue outlier galaxies have been confirmed to be cluster members, with an E+A spectral type. Table 3 shows the three brightest early-type outliers in cluster Cl0016+16 ($z = 0.545$) from the sample of Ellis et al. (1997) (the MORPHS collaboration), who performed the morphological classification with high resolution images from *HST/WFPC2*. All three galaxies have been confirmed to be cluster members as well as featuring an E+A spectral type, obtained either through spectroscopy (Dressler et al. 1999; referred to in the table as MORPHS) or narrowband imaging (Belloni & Röser 1996). The small solid angle covered by *WFPC2* makes meaningless any statistical estimation of field contaminants from morphologically segregated luminosity functions (e.g. Driver et al. 1998).

The comparison of the measured equivalent widths for $H\delta$ with population synthesis models such as BC99 give an age estimate between 0.5 and 2 Gyr for a reasonable range of metallicities $0.2 < Z/Z_{\odot} < 2.5$, with the younger estimates corresponding to the higher metallicities. These estimates are obtained for a model with a single burst. Models with multiple peaks in the star formation rate will yield younger ages for the last major bursting episode. Hence, the ages given above can be taken as upper limits. The population of blue early-type outliers can thus be considered as an important estimator of cluster evolution. A comprehensive study could yield valuable information about the process of galaxy formation in clusters. For instance, if we use the list of early-type galaxies in cluster Cl0016+16 observed by the MORPHS collaboration, and we assume that all spheroids in the red envelope are cluster members, then we can state that down to a completeness magnitude of $F814W < 21.0$,



three out of 25 galaxies are blue outliers, with ages $t < 2$ Gyr, that is with a formation redshift $z_F \lesssim 1$. If we assume a monolithic formation process with a gaussian distribution and a mean at $z_F = 3$, then this 12% fraction will imply a standard deviation of order $\sigma(z_F) \sim 2$, i.e. a rather extended process of star formation. A hierarchical model, where the stellar populations of the faintest galaxies are assembled first, would thus be preferred. This simple calculation shows the power of “outlier statistics”: measurements down to deep completeness magnitudes in a sample of clusters comprising a wide range of redshifts will pose severe constraints on the epochs of star formation. However, we should emphasize that non-spheroidal morphologies might also contribute to the fraction of galaxies that evolve into red envelope early-types. Hence, the simple calculation presented here would only represent a lower limit to the fraction of evolving early-type galaxies, comprising only those that appear already as spheroidal.

8. THE ENRICHMENT OF THE INTRACLUSTER MEDIUM

The intracluster medium (ICM) is a metal-rich hot gas which pervades the central parts of galaxy clusters, and can be detected in X rays via thermal bremsstrahlung radiation. The temperature of this gas is in the range $2 < kT_X < 14$ keV and exceeds the mass of stars in galaxies by a factor of 2 to 10. The metallicity of the ICM is rather high, around $Z_{\odot}/3$, showing no evidence of evolution up to redshifts $z \sim 0.5$ (Mushotzky & Loewenstein 1997). There is a strong correlation between the iron mass content of the ICM and the optical luminosity (Arnaud et al. 1992), a clear sign of a connection between the metallicity of the ICM and the evolution of the early-type population in the cluster. The model described in this paper can be used in order to follow the chemical evolution of the gas and metals being ejected into the ICM. Given the connection found between absolute luminosity — or central velocity

TABLE 3

Blue Outlier Cluster Members in Cl0016+16 ($z = 0.545$)

ID (Morphs)	R.A. (J2000)	Dec. (J2000)	F814W	F555W-F814W	EW($H\delta$) (Å)	z	Source
266	00:18:32.22	16:25:06.6	20.35	2.04	8.5	0.5447	MORPHS
2026	00:18:35.25	16:25:45.1	20.64	2.19	—	0.53	B&R96
809	00:18:31.22	16:26:52.1	20.67	2.06	5.3	0.5304	MORPHS

dispersion, using the Faber-Jackson relation (Faber & Jackson 1976) — and the ejected fraction, we can see that a low mass galaxy with $\sigma = 45 \text{ km s}^{-1}$ or absolute luminosity $M_V = -16.5$, will eject 90% of its content, being practically destroyed right after the first stage of supernova explosions by its massive constituent stars. Therefore, a model for studying the enrichment of the ICM should take into account the contribution from the low mass population of galaxies in the cluster (Dekel & Silk 1986). Note that Mac Low and Ferrara (1999) argue that in thin disk galaxies, winds are effectively suppressed except in very low mass dwarfs; however for the early-type systems we are considering, the spheroidal geometry should render their argument ineffective.

Other mechanisms could also contribute significantly to the metallicity of the ICM. For instance, if we were to consider the merging of disk galaxies with similar masses as precursors of the brightest ellipticals (Toomre & Toomre 1972), then a large

point Z97 show the range in observed magnesium abundances instead.

amount of material (gas, metals and even stars via tidal tails) would be ejected into the intergalactic medium. Furthermore, ram pressure stripping from the hot ICM gas can also play an important role in its enrichment (e.g. Gunn 1989; Evrard 1991). The origin of the metal content in the ICM is not only uncertain with respect to which galaxies contributed the most metals, but the issue of whether most of the metals came from type Ia or type II supernovae is also controversial (see Ishimaru & Arimoto 1997; Gibson, Loewenstein & Mushotzky 1997; Wyse 1997). In our model, we use a fixed ratio of type Ia's with respect to type II's as described in §2, and relate most of the metals in the ICM to ejecta from low mass galaxies. In this section, we will trace only the iron abundance, hence the calculations are insensitive to the parameters related to stars with masses below $M \lesssim 10M_\odot$.

Once the metals and the gas ejected into the ICM from all of the galaxies in the simulated cluster are computed, we need to set a value for the primordial amount of gas in the ICM which is assumed to have zero metal content. This is done by a least squares fit of the model curves compared to observed ICM metallicities from the sample of Mushotzky & Loewenstein (1997), which comprises 21 clusters in the redshift range $0.1 < z < 0.6$, observed with the ASCA X-ray satellite. The primordial mass of ICM gas obtained is roughly 65% regardless of the enrichment models, and the evolution with redshift is shown in figure 8. No clear trend is evident from the data, and the models predict no change in ICM metallicity at moderate-to-high redshifts, mainly caused by the strong star formation efficiency required. The process of chemical enrichment is rather fast, since it is primarily driven by massive OB stars with lifetimes of order a few million years. If formation redshifts $z_F \gtrsim 2$ are assumed for the more abundant component of faint galaxies (which contribute the most to the ICM because of their high ejected fractions), then by $z \sim 1.5$ most of the metals have been released to the intracluster medium, which results in no further evolution of Z_{ICM} . Hence, the lack of evolution in the metal abundance of the ICM observed at moderate redshifts is consistent with a picture where most of the metals are expelled from the population of faint ellipticals. Were recent and big mergers to contribute significantly to the metal abundance of the ICM, then a strong drop in Z_{ICM} should be expected by $z \sim 1-1.5$. Upcoming X-ray observations of clusters with AXAF and XMM will elucidate this point.

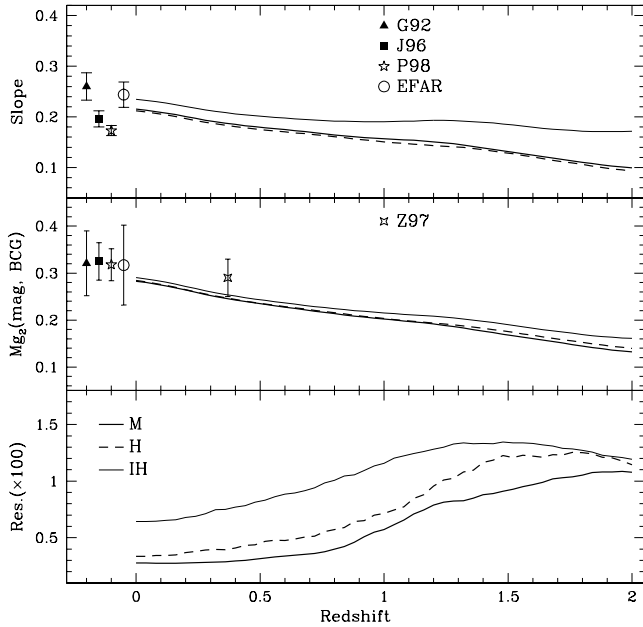


FIG. 7.— Evolution of the magnesium abundance with redshift explored through the correlation between the Lick/IDS Mg_2 index (Worthey 1994) and $\log \sigma$. Notice the observations are systematically above the predicted curves for slope and zero point caused by the magnesium overabundance problem, which enhances the magnesium yields in the central parts of the brightest ellipticals, thereby steepening the slope and increasing the zero point. The data points come from observations of local clusters by Guzmán et al. (1992, G92); Jørgensen et al. (1996, J96); and Colless et al. (1999, EFAR), and of a few clusters at $z \sim 0.37$ from Ziegler & Bender (1997, Z97). The latter only measure a few galaxies so that it is not possible to estimate a slope. Therefore the error bar for

The strong degeneracy between age and metallicity thwarts any attempt at estimating the star formation history of early-type galaxies. Hence, evolutionary studies must include some model in which both age and metallicity are related. A simple chemical enrichment model has been described in this paper, where we have tried to reduce the many factors occurring in galaxy evolution down to the most basic parameters. We believe that infall of gas, outflows from supernova-triggered winds and possible variations in the star formation efficiency can collectively determine chemical enrichment. The results from our simple models demonstrate that outflows can generate the range in metallicity required for the observed color-magnitude relation (figure 1), whereas the other principal parameters, associated with infall of primordial gas or with the star formation efficiency, cannot account for the observations. This agrees with dynamical-spectrophotometric relations such as the Faber-Jackson correlation between central velocity dispersion and absolute luminosity (Faber & Jackson 1976). The ejected fraction of gas should be a function of the mass of the galaxy. It could be argued that there might be a correlation between star formation and galaxy mass so that stars would be preferentially formed in more massive galaxies. This would increase the ejected fraction in these galaxies. However, the color-magnitude diagram would then be strongly altered, bluing the bright end of the red sequence. One way out of this would include other mechanisms “conspiring” to restore the redness of the brightest galaxies. Therefore, we conclude that the simplest explanation for the color-magnitude relation comes from a range of metal abundances caused by the correlation between galaxy mass and ejected fraction. We emphasize that observational evidence concerning this point is still in a primitive stage, and thus a significant age spread cannot be ruled out. However, observations of the Fornax cluster by Kuntschner & Davies (1998) seem to point to a metallicity spread as being responsible for the color-magnitude relation. Other factors such as an IMF with a variable high mass slope or cutoff or variable stellar yields could in principle decrease the effect of outflows on the resulting stellar populations. However, if such factors were to play a significant role in affecting the scatter of the color-magnitude relation, the expected correlation of these factors with galaxy mass should have other observable implications.

The combination of these chemical enrichment tracks with the latest population synthesis models from BC99 allows us to estimate the spectrophotometric properties of cluster early-type galaxies. Using the color-magnitude relation and the luminosity function of local clusters as constraints, clusters can be simulated over a wide range of redshifts for different input parameters and star formation scenarios. A strong degeneracy is found when varying infall parameters (the rate, timescale and delay of infall) or the star formation efficiency. This is just a mapping of the degenerate enrichment tracks shown in figures 1 and 2 with respect to metallicity and $U - V$ color, respectively. Three different star formation scenarios are also considered: monolithic collapse, and two hierarchical models with formation redshifts dependent on the luminosity of the galaxy. The predictions for these models are not as degenerate at high redshifts $z \gtrsim 1$, especially for age-sensitive observables such as the mass-to-light ratio. The most remarkable difference between the models can be shown in the predicted color-magnitude relations in figure 4: hierarchical models (H and IH) clearly display at high redshift a population of early-type galaxies which fall conspicuously

blueward of the “main sequence” red envelope: these blue outliers are so far the best candidates for characterizing cluster evolution. A hierarchical scenario (H-model) presents these outliers as the brightest cluster galaxies, whereas an inverted hier-

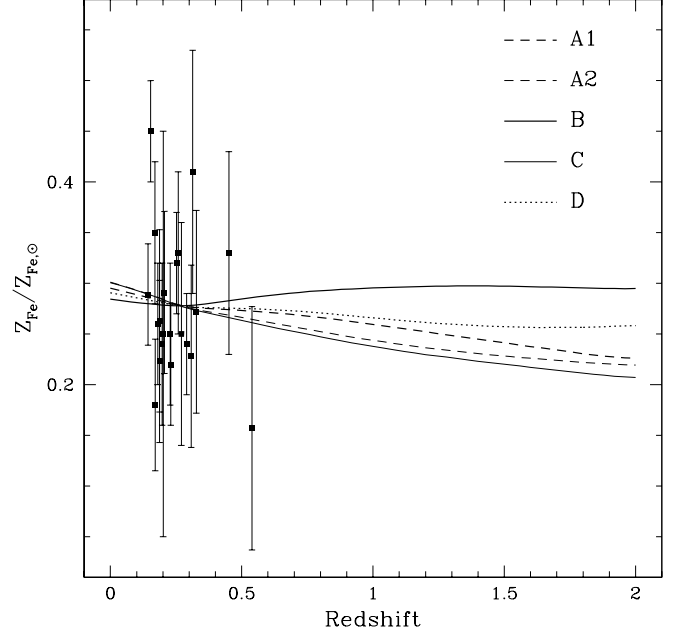


FIG. 8.— Predicted evolution as a function of redshift of the iron content of the intracluster medium from gas ejected from early-type galaxies to a primordial mass of gas which comprises 65% of the present amount in a local rich cluster. The data points come from Mushotzky & Loewenstein (1997). If a significant change in the metallicity of the ICM were eventually detected, a very recent and strong star formation process should be introduced, since most of the metals are produced in massive OB stars with lifetimes of a few million years.

archy (IH-model) identifies them with a faint population of dwarf galaxies. Monolithic collapse results in no major difference in the residuals from the linear fit with respect to luminosity.

A complete sample of three blue outliers down to F814W=21 has been confirmed to be members of cluster Cl0016+16 ($z = 0.545$) using serendipitous observations of these candidates by Belloni & Röser (1996) and the MORPHS collaboration (Dressler et al. 1999). They are also classified as post-starburst (E+A or k+a) galaxies (Dressler & Gunn 1983), a clear sign of recent star formation activity. The observed equivalent widths are matched against the predictions of population synthesis models and an upper limit to the age between 0.5 and 2 Gyr is inferred for a range of metallicities $0.2 < Z/Z_{\odot} < 2.5$, with the younger estimates corresponding to the higher metallicities. This sets an upper limit $z_F \lesssim 1$ on the epoch of formation of these galaxies, favoring a hierarchical clustering scenario where late merging stages could still be associated with significant star formation. It is still a matter of debate whether the spectral signature of young stars in these galaxies corresponds to a large fraction of the galaxy mass. Such quantitative estimates must be performed in order to ascertain whether the star formation process that imprinted the E+A signature on these galaxies played a dominant role in accounting for the observed stellar populations. The evolution of mass-to-light ratios and magnesium abundances can also be explored with these simulated clusters. Both give the same degeneracy for a range of toy enrichment

models, and a significant departure at high redshift ($z \gtrsim 1$) between different star formation scenarios. The comparison between stellar M/L ratios and observations (that trace the total mass) yield a roughly linear correlation between stellar and total matter: $M_{\text{Tot}} \propto M_{\text{St}}^{1.15 \pm 0.08}$.

Given that our model uses outflows as the main cause for the range in colors of cluster early-type galaxies, we can quantify the amount of metals ejected into the intracluster medium (ICM). The top panel of figure 3 shows that a faint galaxy with absolute luminosity $M_V \sim -16$ ejects 85% of its gas. This means that a large number of (dwarf) galaxies contribute significantly to the enrichment of the ICM. This was computed and an initial mass of primordial intracluster gas was assumed. The final value of this initial mass is estimated by comparing the predicted tracks $Z_{\text{ICM}} = Z_{\text{ICM}}(z)$ with cluster X-ray observations from Mushotzky & Loewenstein (1997). A large fraction of the intracluster medium gas must be primordial ($\sim 65\%$) in order to explain these observations. Figure 8 shows that no important evolution in the metal abundance of the ICM is expected up to redshifts $z_F \sim 2$, in rough agreement with the data points. This can be explained because the fraction of metals contributed from ejecta to the ICM is very high even at high redshifts: most

of the metals synthesized in a galaxy come from young stars with lifetimes of order a few million years. Subsequently, intermediate mass stars take over the enrichment process, but they only contribute to a small fraction of the enrichment. Figure 1 shows that any chemical enrichment track using passive evolution results in a sharp rise in metallicities followed by a stable stage in which these metallicities do not change much. Hence, the study of ICM metal abundance in high redshift clusters with forthcoming X-ray telescopes such as *Chandra* and *XMM* will allow us to estimate the role of enrichment from dwarf galaxies or from merger remnants. The latter should translate into a sharp decrease of Z_{ICM} at redshifts $z \gtrsim 1-2$.

We would like to thank Sandra Faber for her very useful remarks and suggestions about this paper and in general about the eternal “tug-of-war” between observations and theories. I.F. acknowledges financial support for this project from the Gobierno de Cantabria, Institut d’Astrophysique de Paris and the Center for Particle Astrophysics at the University of California, Berkeley. J.S. was supported at Berkeley in part by a grant from NASA.

REFERENCES

Arimoto, N. & Yoshii, Y. 1987, *A&A*, 173, 23
 Aragón-Salamanca, A., Baugh, C. M. & Kauffmann, G. 1998, *MNRAS*, 297, 427
 Arnaud, M., Rothenflug, R., Boulade, O., Vigroux, L. & Vangioni-Flam, E. 1992, *A&A*, 254, 49
 Bahcall, N. A. 1996, *astro-ph/9611148*
 Belloni, P. & Röser, H.-J. 1996, *A&AS*, 118, 65
 Blanchard, A., Valls-Gabaud, D. & Mamon, G. A. 1992, *A&A*, 264, 365
 Bower, R. G., Lucey, J. R. & Ellis, R. S. 1992, *MNRAS*, 254, 601
 Cassé, M., Olive, K. A., Vangioni-Flam, E. & Audouze, J. 1998, *New Ast.*, 3, 259
 Colless, M., Burstein, D., Davies, R. L., McMahan, R. K., Saglia, R. P. & Wegner, G. 1999, *MNRAS*, 303, 813
 Dekel, A. & Silk, J. 1986, *ApJ*, 303, 39
 Dressler, A. & Gunn, J. E. 1983, *ApJ*, 270, 7
 Dressler, A. et al. 1999, *ApJ*, In press (*astro-ph/9901263*)
 Driver, S. P. et al. 1998, *ApJ*, 496, L93
 Ellis, R. S., Smail, I., Dressler, A., Couch, W. J., Oemler, A., Butcher, H. & Sharples, R. M. 1997, *ApJ*, 483, 582
 Evrard, A. E. 1991, *MNRAS*, 248, L8
 Faber, S. M. & Jackson, R. 1976, *ApJ*, 204, 668
 Ferreras, I., Charlot, S. & Silk, J. 1999, *ApJ*, 521, 81
 Gibson, B. K., Loewenstein, M. & Mushotzky, R. F. 1997, *MNRAS*, 290, 623
 Gunn, J. E. 1989, in *The epoch of galaxy formation*, p. 167, Frenk, C. S. et al. eds, Kluwer, Dordrecht
 Guzmán, R., Lucey, J. R., Carter, D. & Terlevich, R. J. 1992, *MNRAS*, 257, 187
 Iben, I. & Tutukov, A. 1984, *ApJS*, 54, 335
 Ishimaru, Y. & Arimoto, N. 1997, *PASJ*, 49, 1
 Jørgensen, I., Franx, M. & Kjægaard, P. 1996, *MNRAS*, 280, 167
 Kauffmann, G., White, S. D. M. & Guiderdoni, B. 1993, *MNRAS*, 264, 201
 Kennicutt, R. C. 1998, *ARA&A*, 36, 189
 Kuntschner, H. & Davies, R. L. 1998, *MNRAS*, 295, L29
 Larson, R. B. 1974, *MNRAS*, 169, 229
 Larson, R. B. & Tinsley, B. M. 1974, *ApJ*, 192, 293
 Mac Low, M.-M. & Ferrara, A. 1999, *ApJ*, 513, 142
 Marigo, P., Bressan, A. & Chiosi, C. 1996, *A&A*, 313, 545
 Mabasher, B., Guzmán, R., Aragón-Salamanca, A. & Zepf, S. 1999, *MNRAS*, 304, 225
 Mushotzky, R. F. & Loewenstein, M. 1997, *ApJ*, 481, L63
 Nomoto, K., Iwamoto, K. & Kishimoto, N. 1997, *Science*, 276, 1378
 Pahre, M. A., Djorgovski, S. G. & de Carvalho, R. R. 1998, *AJ*, 116, 1591
 Portinari, L., Chiosi, C. & Bressan, A. 1998, *A&A*, 334, 505
 Prantzos, N. & Silk, J. 1998, *ApJ*, 507, 229
 Press, W. H., Teukolsky, S. A., Vetterling, W. T. & Flannery, B. P. 1992, *Numerical Recipes in C*, Cambridge University Press
 Renzini, A. & Voli, A. 1981, *A&A*, 94, 175
 Sandage, A., Binggeli, B. & Tammann, G. A. 1985, *AJ*, 90, 1759
 Scalo, J. N. 1986, *Fund.Cosm.Phys.*, 11, 1
 Schaller, G., Schaerer, D., Maeder, A. & Meynet, G. 1992, *A&AS*, 96, 269
 Schmidt, M. 1963, *ApJ*, 137, 758
 Scully, S., Cassé, M., Olive, K. A. & Vangioni-Flam, E. 1997, *ApJ*, 476, 521
 Shapiro, S. L. & Teukolsky, S. A. 1983, *Black Holes, White Dwarfs and Neutron Stars*, New York, Wiley-Interscience
 Stanford, S. A., Eisenhardt, P. R. & Dickinson, M. 1998, *ApJ*, 492, 461
 Talbot, R. J. & Arnett, W. D. 1975, *ApJ*, 197, 551
 Thielemann, F. K., Nomoto, K. & Yokoi, K. 1986, *A&A*, 158, 17
 Thielemann, K. F., Nomoto, K. & Hashimoto, M. 1996, *ApJ*, 460, 408
 Tinsley, B. M. 1980, *Fund.Cosm.Phys.*, 5, 287
 Toomre, A. & Toomre, J. 1972, *ApJ*, 178, 623
 Trimble, V. 1995, *PASP*, 107, 1133
 Van den Berg, S. 1962, *AJ*, 67, 486
 Van Dokkum, P. G., Franx, M., Kelson, D. D. & Illingworth, G. D. 1998, *ApJ*, 504, L17
 Visvanathan, N., & Sandage, A. 1977, *ApJ*, 216, 214
 Woosley, S. & Weaver, T. 1995, *ApJS*, 101, 181
 Worthey, G. 1994, *ApJS*, 95, 107
 Wyse, R. F. G. 1997, *ApJ*, 490, L69
 Ziegler, B. L. & Bender, R. 1997, *MNRAS*, 291, 527